Environ. Sci. Technol. **1998**, *32*, 2947−2953

Photochemical Formation of Hydroxyl Radical by Constituents of Natural Waters

PAMELA P. VAUGHAN AND NEIL V. BLOUGH*

Department of Chemistry and Biochemistry, University of Maryland, College Park, Maryland 20742

A new method is employed to determine the rates of photochemical hydroxyl radical (OH) formation in aqueous solutions and in natural waters under both aerobic and anaerobic conditions. Quantum yields for OH formation from the photolysis of nitrate and nitrite obtained by this method are in good agreement with previous measurements. Photolysis of Suwannee River fulvic acid (SRFA) solutions produced the hydroxyl radical under anaerobic conditions in proportion to the SRFA concentration. Under aerobic conditions, the quantum yields for OH formation were slightly higher and exhibited a different wavelength dependence than those obtained under anaerobic conditions. Experiments employing catalase indicate that Fenton chemistry can account for at most 50% of the total signal under aerobic conditions for SRFA irradiated at 310 and 320 nm. These results indicate the presence of a dioxygen-independent pathway of hydroxyl radical production that cannot be assigned to nitrate/nitrite photolysis or to Fenton chemistry. Results from the preliminary application of this method to natural waters are also presented.

Introduction

Numerous studies over the last 15 years have provided unequivocal evidence that OH is generated in natural waters (*1*, *2*) by the photolysis of nitrite (*3*, *4*) and nitrate (5−7), and in waters containing sufficiently high metal ion concentrations, through ligand-to-metal charge-transfer reactions (*8*) and photo-Fenton chemistry (*9*). Recently, however, Mopper and Zhou (*10*, *11*) reported that the total OH production rate in seawaters was significantly larger than that expected from the sum of these processes. They concluded that there was a "missing source" of hydroxyl radical production and that this source was most likely due to the direct photolysis of (colored) dissolved organic matter (CDOM).

However, these past studies did not examine isolated CDOM (e.g., Suwannee River fulvic acid) that had been stripped of nitrite, nitrate, and metal ions. Furthermore, because most of the OH detection methods that have been employed in the past require the presence of dioxygen to work properly, these methods were incapable of determining whether dioxygen was required for OH production.

Here, we apply a new method that can be used to quantify OH production rates both in the presence and the absence of dioxygen (see Scheme 1). This method employs the reaction between OH and dimethyl sulfoxide (DMSO) to produce quantitatively a methyl radical (*12*), which then reacts with an aminonitroxide (either **I** or **Ia**; see Scheme 1) (*13*−*16*) to produce a stable *O*-methylhydroxylamine (**II** and **IIa**). Following derivatization with fluorescamine (**III**), the *O*-methylhydroxylamine **IV** (or **IV**a) is separated by reversed-phase high-performance liquid chromatography (HPLC) and quantified fluorometrically. Application of this method to solutions of nitrate and nitrite confirm previous measurements of quantum yields for OH production. Using this method with solutions of SRFA, a dioxygen-independent source of OH that cannot be attributed to nitrite or nitrate photolysis or to Fenton chemistry is revealed. Preliminary application of this method to natural waters shows higher quantum yields for OH production and a slightly different wavelength dependence than that of SRFA, indicating possible additional contributions from the photolysis of nitrate or nitrite and photo-Fenton chemistry.

Experimental Section

Chemicals. Boric acid (99.999%), sodium phosphate, sodium hydroxide (99.99%), dimethyl sulfoxide (DMSO) (99.9%), hydrogen peroxide, potassium oxalate, 1,10-phenanthroline, and 3-aminomethyl-2,2,5,5,-tetramethyl-1-pyrrolidinyloxy free radical (3-amp) were purchased from Aldrich. Fluorescamine and a stock solution of bovine liver catalase (3.08×10^5 units/mL) were purchased from Sigma. Chloroform, ferrous sulfate, and potassium nitrite were purchased from J. T. Baker. Sodium nitrate, HPLC grade methanol, acetonitrile, and glacial acetic acid were purchased from Fisher. 3-Amino-2,2,5,5,-tetramethyl-1-pyrrolidinyloxy free radical (3-ap) was purchased from Fisher (Acros). Suwanee River fulvic acid (SRFA) was obtained from the International Humic Substances Society (IHSS). All chemicals were used as received with the exception of the 3-amp (see below). A Millipore Milli-Q system provided water for all experiments.

Fluorescamine solutions (5 mM) were prepared daily in acetonitrile and stored in the dark at room temperature. HPLC mobile phase was prepared from glacial acetic acid and Milli-Q water with the pH adjusted using sodium hydroxide. Stock SRFA solutions were prepared in pH = 8, 0.2 M borate buffer every 2−3 months and were stored in dark bottles at 4 °C. Nitrite and nitrate solutions were made in 50 mM borate buffer at pH = 8 every few weeks and stored in the dark at 4 °C. Natural water samples were obtained from the surface water pumping system of the R/V *Cape Henlopen* and passed through a 0.2-μm Gelman fluted filter. Samples were stored in the dark at 4 °C.

Apparatus. Absorption spectra were obtained with a Hewlett-Packard 8452A diode array spectrophotometer. The HPLC system was identical to that described previously (*13*, *17*). Chromatographic separations were carried out at room temperature with a flow rate of 1 mL/min. Separations were performed isocratically using a mobile phase composition of 65% methanol/35% sodium acetate (50 mM, pH = 4.0). A 50-μL injection loop was used for all experiments. Total iron content of the SRFA standard was determined using a Perkin-Elmer 2380 flame atomic absorption spectrometer. The iron content of a 20 mg/L SRFA solution was below the detection limit for this instrument (<3.5 μM Fe). Nitrite and nitrate analyses were performed at Horn Point Environmental Laboratory on a 20 mg/L SRFA solution using a standard colorimetric technique (*18*). Analysis of an older solution (3 months) yielded 0.15 μM nitrite and 1.51 μM nitrate. Fresh solutions yielded 0.15 μM nitrite and 0.41 μM nitrate.

Purification of I. The 3-amp (**I**) was purified by reversed-phase HPLC using a Waters C_{18} column, employing isocratic elution with 70% (50 mM acetate buffer, pH = 4.0)/30%

* Corresponding author e-mail: nb41@umail.umd.edu; fax: (301) 314-9121.

S0013-936X(97)01041-9 CCC: $15.00
Published on Web 06/17/1998

SCHEME 1

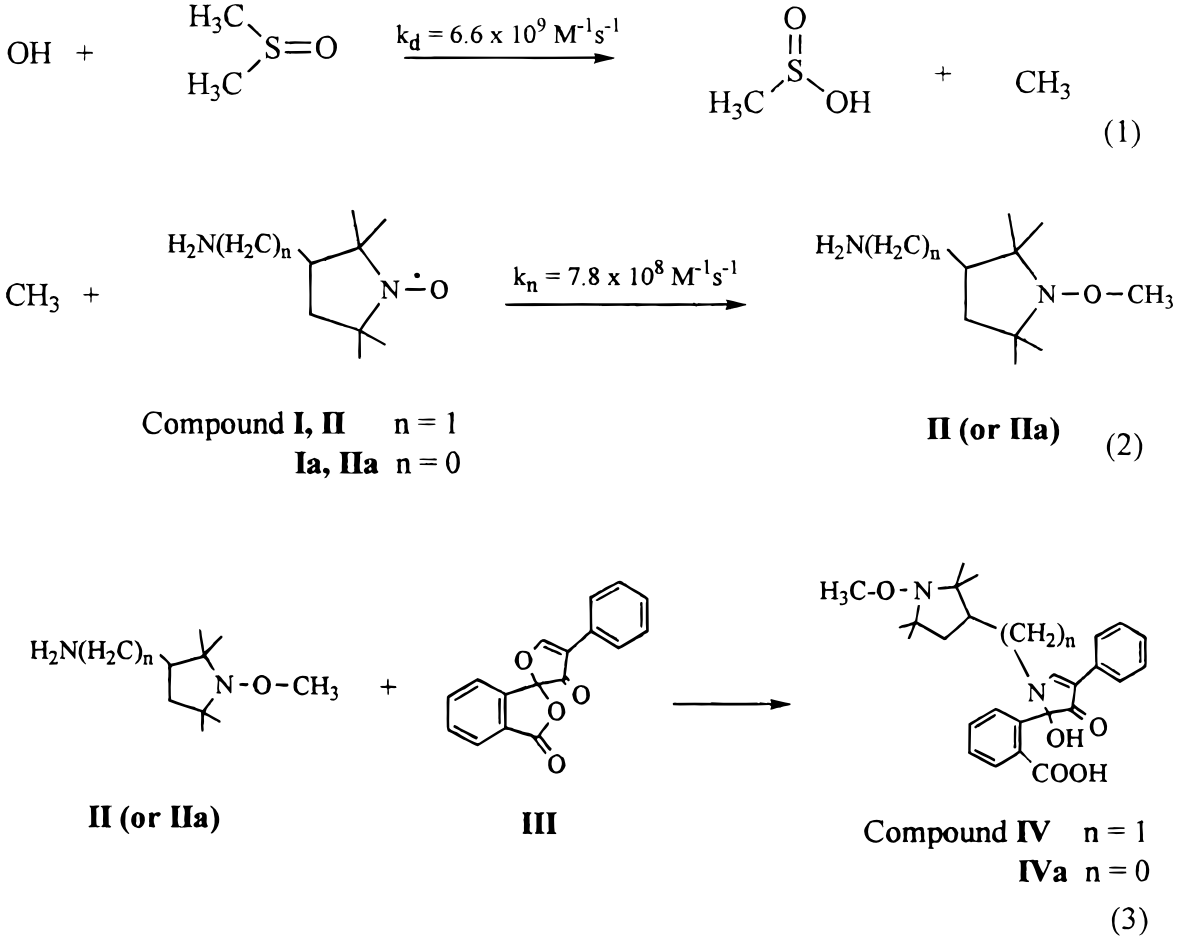

methanol mobile phase. A Spectroflow model 757 absorbance detector, set to 425 nm, was used to monitor the eluent. Three guard columns (Upchurch, 2 mm i.d. × 2 cm) connected in series with PEEK tubing (i.d. 0.02 in.) served as the HPLC injection loop. Each column was packed with C_{18} Sep-Pak material and activated by flushing with methanol for 15-min followed by a 15 min flush with Q water. A 20 mM solution of **I** was prepared by suspending 25 mg of **I** in 7.5 mL of Milli-Q water. This solution was vortexed for 1 min and then filtered using a 0.2-μm nylon filter. Approximately 0.4 mL of this solution was slowly loaded onto the injection loop. **I**, with a retention time of 3 min, was collected directly into a centrifuge tube. The pH of the sample was raised to 13 using sodium hydroxide, and **I** was extracted into chloroform, which was subsequently rinsed two times with pH 13 Milli-Q water. The chloroform phase was transferred to a round-bottom flask and rotoevaporated to a yellow oil. This procedure was sometimes repeated, and portions of the chloroform phase were pooled together and evaporated in the same flask. The oil was dissolved in 50 mM borate buffer (pH = 8.0). Aliquots were dispensed into plastic Eppendorf microcentrifuge tubes and were stored at −20 °C.

During the course of this investigation, we observed that 3-ap obtained from Fisher was significantly and consistently purer than the 3-amp obtained from Sigma. Since the use of 3-ap provided results that were identical to those of the 3-amp without the need for purification (see below), 3-ap was used in the latter portion of this work and is suggested for use in all future studies.

Calibration of IV and IVa. **IV** and **IVa** were prepared via the Fenton reaction by methods described previously (*17*). **IV** or **IVa** was dissolved in a small volume of DMSO and then diluted into pH = 8.0, 50 mM borate buffer. The concentration of the stock was determined spectrophotometrically at 386 nm (ϵ_{386} = 5225 M^{-1} cm^{-1}). A Hitachi model L-7480 fluorescence detector, set to 390 nm (excitation, 15 nm band-pass) and 490 nm (emission, 15 nm band-pass), was used to monitor the eluent. A standard curve of fluorescence peak area versus the concentration of **IV** or **IVa** injected into the HPLC was then generated by the serial dilution of **IV** or **IVa**. The fluorescence response increased linearly with concentration over the range from 5 to 2000 nM (n = 7). For all calibration curves, r^2 > 0.998, and y-intercepts were not significantly different from zero. The detection limit was estimated as that concentration corresponding to a signal twice the standard percent relative error (±10%) of the background obtained at a particular wavelength (see below). For example at 295 nm, the background was substantial (∼220 nM) and the detection limit was estimated to be ∼45 nM, whereas at 343 nm the background becomes negligible and a detection limit of ∼8 nM was estimated.

Irradiation Conditions. Typically, 1 mM nitrite and nitrate samples (in 50 mM borate buffer; pH = 8) were prepared in a 1-cm cuvette containing appropriate concentrations of DMSO and usually 50 μM **I** or **Ia** under anaerobic conditions and 250 μM **I** or **Ia** under aerobic conditions. Samples containing appropriate concentrations of SRFA in 50 mM borate buffer, pH = 8, were prepared in a similar fashion. Samples containing SRFA and catalase were prepared and kept in the dark for 5 min to allow for any residual peroxides to be consumed by the catalase before addition of the probe (**I** or **Ia**) and DMSO. Natural waters were irradiated at their original pH (7−7.5) following the addition

of **I** or **Ia** and DMSO; the pH was then adjusted to 8.0 prior to derivatization with fluorescamine. All anaerobic samples were bubbled with argon for 5 min prior to irradiation, and the headspace was continuously flushed during the irradiation. Following irradiation for an appropriate length of time (10 min for nitrate and nitrite solutions, 20 min for SRFA solutions, and 20 min to 2 h for natural water solutions), 1 mL of sample was derivatized with 200 μL of 5 mM fluorescamine, with 50 μL of this solution then injected onto the HPLC.

The output of a 1000-W Hg−Xe arc lamp was passed through a Spectral Energy GM 252 monochromator set to a band-pass of 10 nm and directed onto the 1-cm quartz cell containing 3 mL of the sample solution. Rates of OH production were acquired from the peak area of the product (**IV** or **IVa**) following subtraction of the peak area obtained for an irradiated blank containing identical concentrations of the nitroxide and DMSO alone. Light intensities were measured using an International Light research radiometer model IL1700 and calibrated using the potassium ferrioxalate actinometer described by Hatchard and Parker (*19*). The amount of Fe(II) formed in the actinometer was determined spectrophotometrically following chelation with 1,10-phenanthroline, using a standard curve generated with known amounts of ferrous sulfate and 1,10-phenanthroline (*20*). Apparent quantum yields were calculated using

$$\Phi = \frac{RP}{0.588 I_0 (1 - 10^{-A})} \quad (1)$$

where R is the rate of OH production (in molecules cm^{-3} s^{-1}), P is the path length of the cell (1 cm), I_0 is the lamp intensity at the surface of the cell (in photons cm^{-2} s^{-1}) acquired from the radiometer reading, A is the initial absorbance of the solutions at the irradiation wavelength, and the factor 0.588 accounts for the difference between the radiometric and actinometric measurements. Less than 10% of the original absorbance was lost over the time courses of the irradiations.

Results and Discussion

Background from Nitroxide and DMSO. Preliminary experiments revealed that irradiation of solutions containing only DMSO and nitroxide (either **I** or **Ia**) produced small amounts of the methyl radical adduct (**IV** or **IV**a; Figure 1, peak at 10.5 min). The yield of this adduct increased with increasing concentration of **Ia** and with decreasing wavelength, but in the presence of high levels of DMSO, it was independent of the DMSO concentration. Adding excess ethanol (up to 800 mM) to a solution containing 10 mM DMSO and 500 μM **Ia** eliminated the formation of this adduct. These results indicate that this background arises from small amounts of photochemically generated OH in the solutions containing the nitroxides. This background appears to arise from a trace UV-absorbing contaminant introduced with the nitroxide, since irradiation of the lower energy band of **Ia** (398 nm) did not produce this adduct.

Because photolysis of the nitroxide solutions at short wavelengths (<310 nm) produced a background unrelated to OH formation by the photolytic processes of interest, this signal was always subtracted from the total adduct yield (Figures 1 and 2). The highest background due to this process was observed at the shortest irradiation wavelength of 290 nm and was never more than 50% of the signal observed in the presence of CDOM. Samples containing only CDOM and **I** produced a light blank that was usually less than 4% of the signal observed in the presence of both CDOM and DMSO. This amount of methyl radical adduct, produced by the direct photolysis of CDOM (SRFA), was consistent with

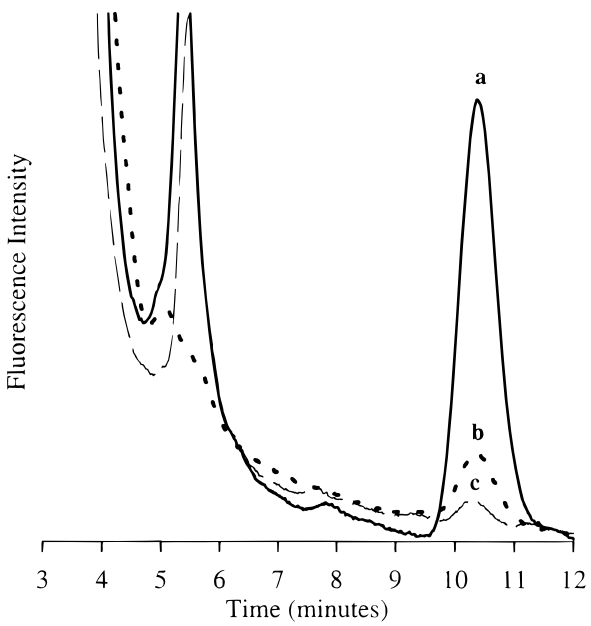

FIGURE 1. Chromatograms illustrating the production of IV (peak at 10.5 min) following irradiation of blank and sample solutions for 20 min at 310 nm. Formation rates of IV were obtained from a solution containing 15 mg/L SRFA, 50 μM I, and 10 mM DMSO (a, —); I and DMSO (b, ---) alone; SRFA and I (c, — —) alone. All reactions were performed anaerobically in pH = 8, 50 mM borate buffer using a lamp intensity of 4.9 × 10^{-3} W cm^{-2}.

that observed in past studies (*1*, *13*), as was the levels of production of the acetyl radical adduct (Figure 1, peak at 5.5 min). The slight variations in retention times of the radical adducts between this (Figures 1 and 2) and previous studies (*17*, *21*) is attributed to small differences in mobile phase composition and column performance. The identity of the adducts was always confirmed by coelution with standards as well as by other control experiments (see below).

Nitrite and Nitrate Photolysis. To test this new method, we examined the production of OH by the photolysis of nitrite (*3*, *4*) and nitrate (*5*−*7*):

$$NO_2^- + h\nu \rightarrow NO + O^- \quad (2)$$

$$NO_3^- + h\nu \rightarrow NO_2 + O^- \quad (3)$$

$$O^- + H_2O \rightarrow OH + OH^- \quad (4)$$

Under *anaerobic* conditions, irradiation of 1 mM nitrite for 10 min at 310 nm in the presence of 10 mM DMSO and 50 μM **Ia** produced one major product with an elution time identical to that of authentic **IVa** (Figure 2, peak at 11.5 min). This product was largely eliminated upon removal of either the DMSO or the nitrite, providing additional evidence that the product was indeed **IVa** (Scheme 1). Increasing the concentration of **Ia** from 50 to 600 μM did not increase the yield of **IVa**, indicating that the methyl radical was quantitatively scavenged by **Ia** over this concentration range (data not shown).

To determine the concentration of DMSO needed for quantitative scavenging of the OH radical, the dependence of the formation rate of **IVa** on DMSO concentration was examined under anaerobic conditions (Figure 3). This rate exhibited a hyperbolic dependence on DMSO concentration, with quantitative scavenging evident at DMSO concentrations above 10 mM. Under the conditions of this experiment (1 mM nitrite), the major competitive sink of OH is the reaction with nitrite:

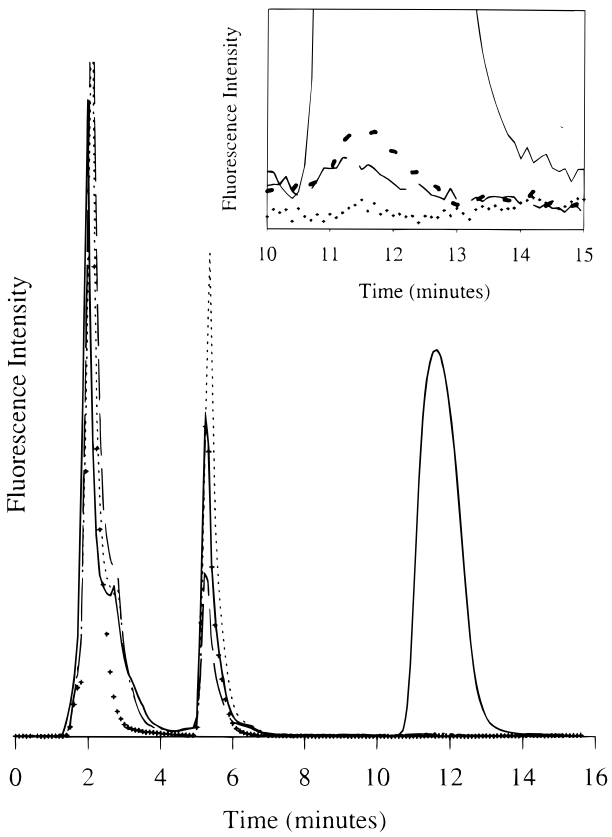

FIGURE 2. Chromatograms illustrating the production of IVa (peak at 11.5 min) following irradiation of blank and sample solutions for 10 min at 310 nm. Formation rates of IVa were obtained from a solution containing 1 mM nitrite, 50 μM Ia, and 10 mM DMSO (—); Ia and DMSO (---) alone; nitrite and Ia (— —) alone; nitrite and DMSO (+) alone. All reactions were performed anaerobically in pH = 8, 50 mM borate buffer using a lamp intensity of 1.4 × 10^{-3} W cm^{-2}.

$$\xrightarrow[h\nu]{k_f} OH \quad \begin{cases} + NO_2^- \xrightarrow{k_{NO_2} = 1.1\times10^{10}} OH^- + NO_2 & (5) \\ + DMSO \xrightarrow{k_d = 6.6\times10^{9}} CH_3 + CH_3SOOH & (6) \end{cases}$$

In this case, the initial rate of the formation of **IVa** is given by

$$R = \left(\frac{d(\mathbf{IV})}{dt}\right)_0 = \frac{k_f k_d[DMSO]}{k_d[DMSO] + k_{NO_2}[NO_2^-]} \qquad (7)$$

which predicts a hyperbolic dependence of the formation rate (R) of **IV** on DMSO concentration, consistent with the experimental data (Figure 3). A linear form of this relation can be obtained by taking the reciprocal of eq 7 (see inset Figure 3)

$$\frac{1}{R} = \frac{1}{k_f} + \frac{k_{NO_2}[NO_2^-]}{k_d k_f}\frac{1}{[DMSO]} \qquad (8)$$

with the slope (S) and intercept (In) given by

$$S = \frac{k_{NO_2}[NO_2^-]}{k_d k_f} \qquad (9)$$

$$\ln = \frac{1}{k_f} \qquad (10)$$

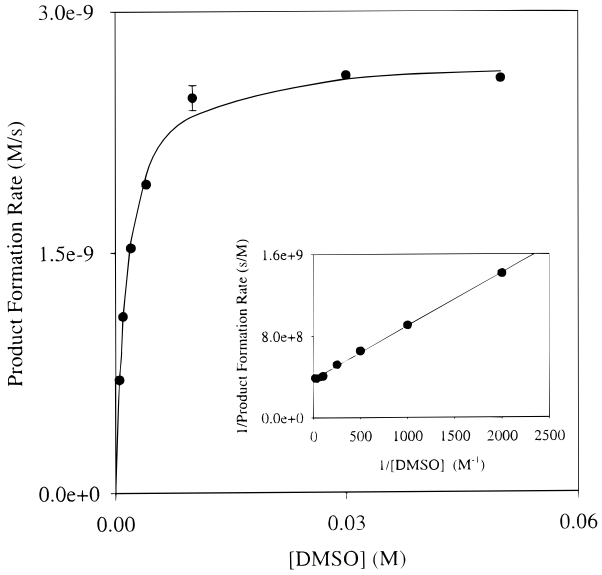

FIGURE 3. Dependence of the formation rate of IVa on DMSO concentration. Formation rates of IVa were obtained from a solution containing 1 mM nitrite and 50 μM Ia. All reactions were performed anaerobically at 310 nm in pH = 8, 50 mM borate buffer using a lamp intensity of 1.44 × 10^{-3} W cm^{-2}. The solid line represents the hyperbolic curve generated from the values of the slope and intercept obtained from a linear least-squares fit to a double-reciprocal plot of the data (inset, see text).

Employing the known $[NO_2^-]$ = 1 mM, the data from Figure 3 (inset; $S = 5.23 + 0.08 \times 10^5$ and In = $3.75 \pm 0.07 \times 10^8$) can be used in eqs 9 and 10 to calculate k_{NO_2}/k_d, the rate constant ratio of the reaction of OH with nitrite and DMSO, respectively. This ratio, 1.4, is in good agreement with the expected rate constant ratio, $k_{NO_2}/k_d = 1.7$, calculated from the known rate constants for the reaction of OH with nitrite (1.1×10^{10} M^{-1} s^{-1}) and DMSO (6.6×10^9 M^{-1} s^{-1}) (*22*). This result provides very strong evidence that OH is indeed the species giving rise to the methyl radical through reaction with DMSO.

Under *aerobic* conditions, dioxygen will compete with the nitroxide for the methyl radical

$$\xrightarrow{k_f} CH_3 \quad \begin{cases} + O_2 \xrightarrow{k_o} CH_3O_2 & (11) \\ + I\ (\text{or Ia}) \xrightarrow{k_n} II\ (\text{or IIa}) & (12) \end{cases}$$

thus leading to an expression analogous to that presented above:

$$R = \left(\frac{d(\mathbf{IV})}{dt}\right)_0 = \frac{k_n k_f[\mathbf{I}]}{k_o[O_2] + k_n[\mathbf{I}]} \qquad (13)$$

which predicts a hyperbolic dependence of the formation rate (R) of **IV** on nitroxide concentration, consistent with the experimental results (Figure 4). Assuming an $[O_2] = 250\ \mu$M, the parameters obtained from a nonlinear least-squares fit of the data to a hyperbolic curve can be used to determine the rate constant ratio for the reaction of O_2 and **I** (or **Ia**) with the intermediate radical. This ratio ($k_o/k_n = 4.4 \pm 0.8$) is equivalent, within experimental error, to that obtained in a previous study ($k_o/k_n = 3.6 \pm 0.8$) (*17*) and is in reasonable agreement with values calculated from the known rate constants for the reaction of the methyl radical with O_2 (4.7×10^9 M^{-1} s^{-1}) (*23*) and a related nitroxide (7.8×10^8 M^{-1} s^{-1}) (*24*), $k_o/k_n = 6.0$.

Because O_2 is the only significant competitive sink of the methyl radical under aerobic conditions, the production rate

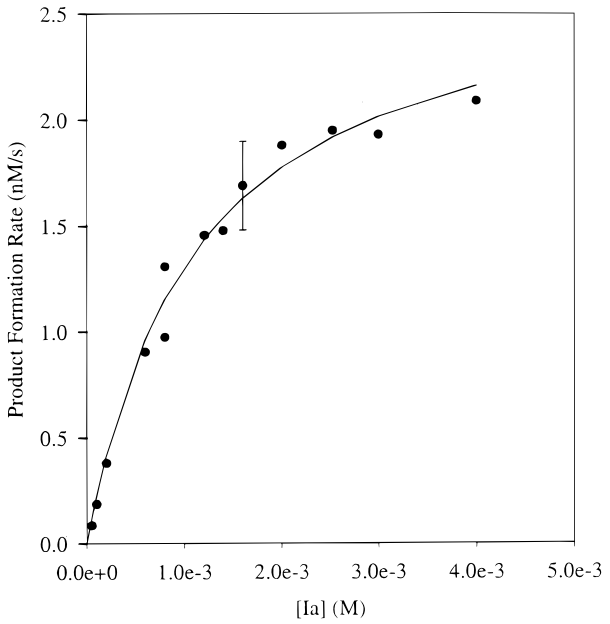

FIGURE 4. Dependence of the formation rate of IVa on the concentration of Ia under aerobic conditions. Conditions were as in Figure 3, except [DMSO] = 10 mM and a lamp intensity of 1.9 × 10^{-3} W cm^{-2} was used. The solid line represents a nonlinear least-squares fit to the data.

(R) can be corrected to k_f using a rearranged form of eq 13:

$$k_f = R\left(1 + \frac{k_o[O_2]}{k_n[\mathbf{I}]}\right) \qquad (14)$$

where R is the measured formation rate of **IV** at a known concentration of **I**, and $([O_2]k_{o)}/k_n$ is obtained from the data in Figure 4. R has been corrected to k_f when OH formation rates or quantum yields are reported for aerobic conditions [($k_f = 5.4 + 0.8R$) at 250 μM **I**].

Employing conditions that would ensure the quantitative detection of OH (deaeration and a 15-fold excess of DMSO over nitrite), we determined the quantum yields for photolysis of nitrite (1 mM) in 50 mM borate buffer (pH = 8.0). Values obtained at 354 nm ($\Phi_{354} = 0.029 \pm 0.005$) and at 308 nm [$\Phi_{308} = 0.062 \pm 0.005$ (anaerobic), 0.059 ± 0.005 (aerobic, following correction using eq 15)] were in good agreement with values previously reported by Zafiriou and Bonneau ($\Phi_{354} = 0.02 \pm 0.01$) (*4*) and Zellner et al. ($\Phi_{308} = 0.071$) (*7*). To test further our ability to measure hydroxyl radical production between 290 and 300 nm, the quantum yields for the photolysis of nitrate (1 mM) in deaerated borate buffer containing 10 mM DMSO were obtained. Values acquired at 290 nm (0.010 ± 0.002), 295 nm (0.011 ± 0.002), and 300 nm (0.009 ± 0.002) were in agreement with those determined by Jankowski and Kieber using another method ($\Phi_{290} = 0.012 \pm 0.001$; $\Phi_{295} = 0.010 \pm 0.001$; $\Phi_{300} = 0.008 \pm 0.001$).

OH Production by SRFA. Irradiation of deaerated solutions of SRFA containing DMSO and **I** (or **Ia**) produced **IV** (**IVa**) in yields much greater than those observed in the absence of DMSO or SRFA (Figure 1). Under anaerobic conditions, increasing the concentration of **I** (**Ia**) from 10 to 600 μM did not increase the yield of **IV** (**IVa**), indicating that the methyl radical was scavenged quantitatively.

To determine the lowest concentration of DMSO adequate for the quantitative scavenging of OH, the dependence of the formation rate of **IV** (**IVa**) on DMSO concentration was again determined (Figure 5). This experiment showed that a quantitative reaction could be attained at [DMSO] ≥ 10 mM, even for the highest concentration of SRFA tested (10 mg/L).

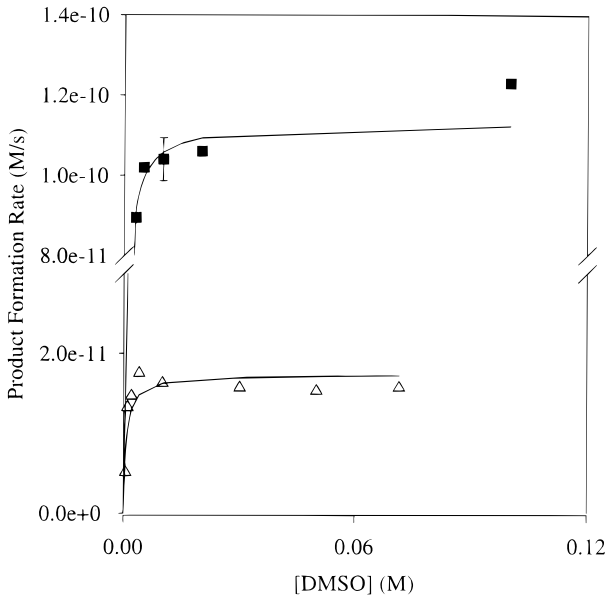

FIGURE 5. Dependence of the formation rate of IV or IVa on DMSO concentration. Product formation rates were obtained from a solution containing 10 mg/L SRFA and 50 μM I (■), 310 nm, lamp intensity of 4.9 × 10^{-3} W cm^{-2}; 10 mg/L SRFA and 50 μM Ia (△), 310 nm, lamp intensity of 1.48 × 10^{-3} W cm^{-2}. All reactions were performed anaerobically in pH = 8, 50 mM borate buffer. The solid line indicates a nonlinear least-squares fit to the data.

Under anaerobic conditions, a linear relationship was observed between the rate of OH production and SRFA concentration, suggesting that the SRFA is the source of the OH and that dioxygen is not required for OH formation. This linear relationship was observed for irradiation at both 310 and 320 nm (Figure 6).

The wavelength dependence of the quantum yields (Φ) for hydroxyl radical production in the presence and the absence of dioxygen exhibited similar though not identical behavior (Figure 7). Under anaerobic conditions, the quantum yields decreased precipitously between 340 and 350 nm, falling below our detection limit by 350 nm, whereas the yields obtained under aerobic conditions remained well above the detection limit at wavelengths extending to 360 nm. At wavelengths between 310 and 330 nm, the quantum yields were similar in magnitude to those previously reported by Mopper and Zhou for coastal waters (*10*, *11*). However, unlike Mopper and Zhou, who observed a substantial increase in quantum yields at $\lambda < 310$ nm for natural waters, we saw a decrease in both aerobic and anaerobic yields for SRFA. This difference does not result from our limited sensitivity in this wavelength regime. Using Mopper and Zhou's values for the quantum yields at $\lambda < 310$ nm leads to the prediction of signals well above the backgrounds at these wavelengths.

In principle, contamination by low levels of dioxygen in the deaerated samples could lead to the formation of H_2O_2 and thus OH through the Fenton reaction:

$$Fe(II) + H_2O_2 \rightarrow Fe(III) + OH + OH^- \qquad (15)$$

To test this possibility, as well as to determine if H_2O_2 was contributing significantly to OH production in aerated samples, catalase was added to both aerated and deaerated samples to remove H_2O_2. With irradiation at 320 nm (Table 1), the rate of OH formation in deaerated samples containing 80 units/mL catalase decreased by no more than 10%; whereas for aerated samples, the OH formation rate was halved. Similarly, irradiation of deaerated solutions at 310 nm (Table 2) in the presence of 50 units/mL catalase produced

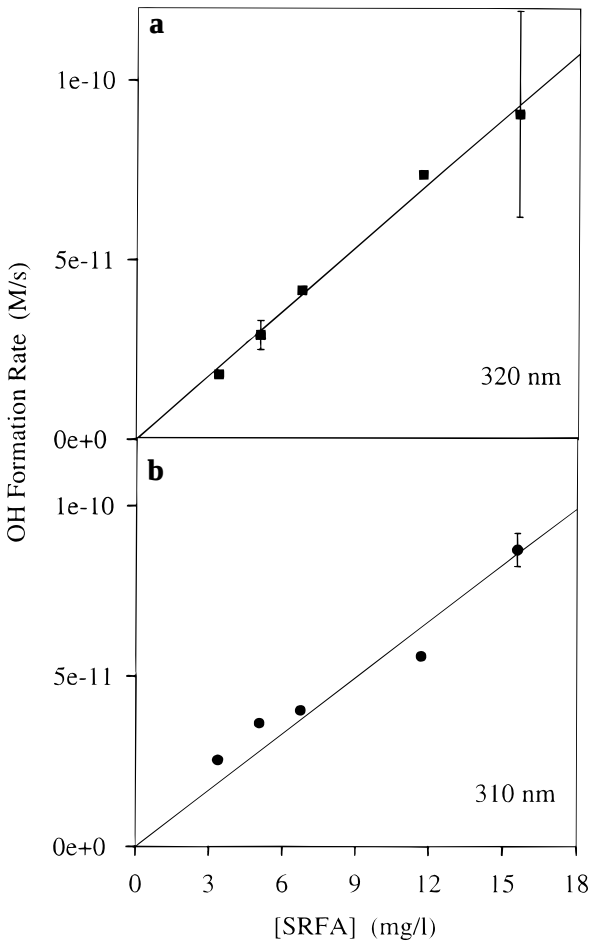

FIGURE 6. Dependence of the formation rate of IV on the concentration of SRFA. Product formation rates were obtained from a solution containing 50 μM I and 10 mM DMSO at irradiation wavelengths of 320 nm (■, a) and 310 (●, b). All reactions were performed anaerobically in pH = 8, 50 mM borate buffer using lamp intensities of 2.9×10^{-3} W cm^{-2} at 320 nm and 4.8×10^{-3} W cm^{-2} at 310 nm.

TABLE 1. Catalase Experiments Using I

	rate (M/s)[a]	rate + cat[b]	rate + cat[c]
aerobic	$2.4 \pm 0.3 \times 10^{-11}$	1.3×10^{-11}	
anaerobic	2.1×10^{-11}	1.9×10^{-11}	1.9×10^{-11}

[a] Samples containing 50 μM **I**, 10 mM DMSO, and 10 mg/L SRFA were irradiated 20 min at 320 nm (lamp intensity = 1.23×10^{-3} W cm^{-2}). [b] 40 units/mL catalasec. [c] 80 units/mL catalase.

TABLE 2. Catalase Experiments Using Ia

	rate (M/s)[a]	rate + cat[b]	rate + cat[c]
aerobic	$2.2 \pm 0.7 \times 10^{-11}$		$1.2 \pm 0.3 \times 10^{-11}$
anaerobic	1.6×10^{-11}	9.7×10^{-12}	$1.05 \pm 0.05 \times 10^{-11}$

[a] Samples containing 50 μM **Ia**, 10 mM DMSO, and 10 mg/L SRFA were irradiated 20 min at 310 nm (lamp intensity = 1.83×10^{-3} W cm^{-2}). [b] 26 units/mL catalase. [c] 49 units/mL catalase.

a 30% decrease in the OH formation rate, while the aerobic rate decreased by almost half and became similar in magnitude to the rate obtained under deaeration. These results indicate that the level of OH formation observed under anaerobic conditions cannot be attributed to the Fenton reaction and further suggests that the Fenton reaction contributes no more than ~50% to the total OH formation

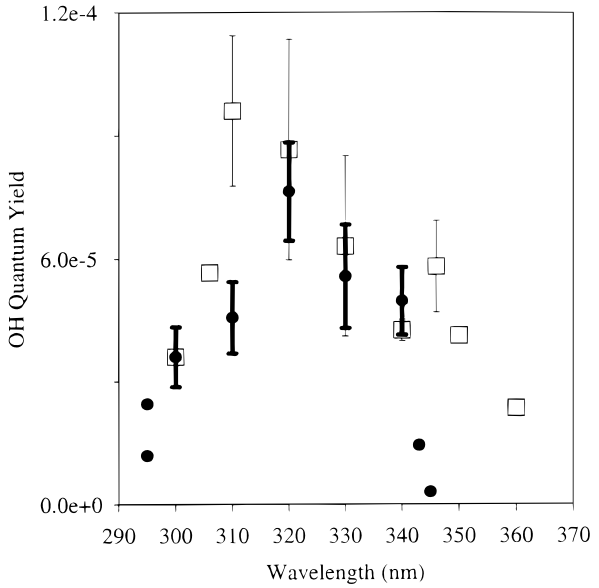

FIGURE 7. Wavelength dependence of the quantum yield for SRFA under aerobic (□) and anaerobic (●) conditions. Anaerobic samples in 50 mM borate buffer (pH = 8) solution contained 50 μM I, 10 mM DMSO, and 10 mg/L SRFA. Aerobic samples contained 250 μM I and identical concentrations of DMSO and SRFA.

TABLE 3. Natural Water Quantum Yields

	Chesapeake Bay Mouth[a] lat. 37°0.1673′ long. 76°2.8917′	Upper Delaware Bay[b] lat. 39°48.0940′ long. 75°24.4972′	Upper Delaware Bay[c] lat. 39°32.79′ long. 75°32.73′
aerobic	6.0×10^{-4}	1.6×10^{-4}	$2.0 \pm 0.5 \times 10^{-4}$
anaerobic	1.1×10^{-4}	2.3×10^{-4}	$3.0 \pm 0.6 \times 10^{-4}$

[a] Anaerobic samples contained 50 μM **Ia**, whereas aerobic samples contained 250 μM **Ia** and 600 mM DMSO. Irradiations were for 2 h at 320 nm. Water collection date 6/3/97. [b] Same as above except 50 mM DMSO was used and irradiations were for 1 h. Water collection date 6/3/97. [c] Same conditions as footnote *b*. Water collection date 8/30/96.

rate at these wavelengths. Furthermore, the anaerobic production of OH cannot be assigned to nitrite or nitrate photolysis; OH formation rates calculated from the known nitrite and nitrate concentrations in these solutions can account for no more than 1% of the total adduct yield. These results argue that the anaerobic production of OH in solutions of SRFA arises from the direct photolysis of the organic matter through a dioxygen-independent pathway, consistent with a previous suggestion by Mopper and Zhou (*10*, *11*).

OH Production in Natural Waters. Preliminary application of this method to natural waters revealed significantly higher apparent OH quantum yields (Table 3) and a slightly different wavelength dependence than that observed for SRFA (Figures 7 and 8). Apparent quantum yields determined at 320 nm for waters from the Chesapeake Bay mouth and from the upper Delaware Bay were similar in magnitude (~$2-6 \times 10^{-4}$; Table 3). However, the apparent quantum yield acquired for surface waters from the bay mouth under aerobic conditions was significantly higher than that obtained anaerobically, indicating the presence of Fenton chemistry (eq 16) or of another dioxygen-dependent pathway for OH production. In contrast, apparent OH quantum yields obtained for waters at the head of the Delaware Bay under aerobic conditions, although higher than that obtained for SRFA, were significantly lower than the value for the Chesapeake sample and, more surprisingly, appeared to be slightly lower than the values obtained anaerobically (Figure

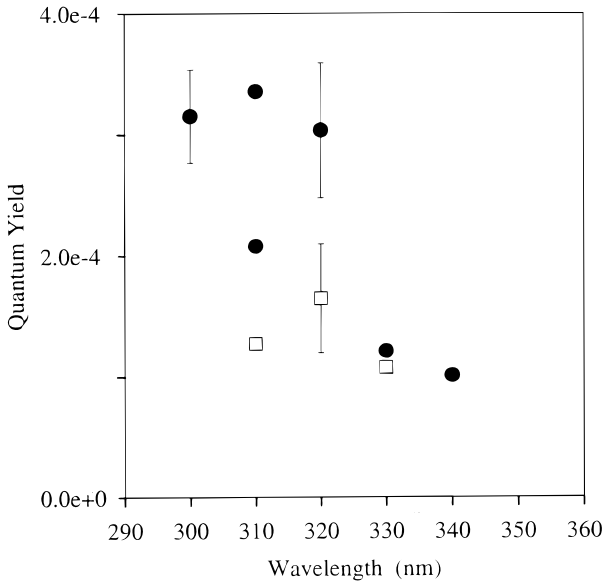

FIGURE 8. Wavelength dependence of the quantum yield for Delaware water under aerobic (□) and anaerobic (●) conditions. Conditions were as in Figure 7, except [DMSO] = 50 mM. Water collected at latitude 39°32.79′ and longitude 75°32.73′ on 8/30/96.

8, Table 3). Given the uncertainties in these measurements, however (Figure 8), the values obtained under aerobic and anaerobic conditions for the Delaware samples may, in fact, be identical. Thus in contrast to the Chesapeake sample, OH production in the Delaware samples appears to be dominated by dioxygen-independent mechanism(s) such as nitrite or nitrate photolysis or through the direct photolysis of the CDOM as observed for the SRFA (see above). Interestingly, samples obtained at nearby positions within the Delaware Bay in successive years showed similar quantum yields.

We have described a new method for determining the rates of photochemically generated OH production that can be used under both aerobic and anaerobic conditions, thus allowing some insight into the mechanisms of OH production. Because higher concentrations of **I** (or **Ia**) are needed under aerobic conditions to obtain a reasonable yield in the presence of dioxygen, the higher backgrounds at shorter wavelengths may limit the sensitivity of the method in this regime. Thus, this method may not be feasible under aerobic conditions when the photochemical formation rates are very low and where higher concentrations of **I** (or **Ia**) are needed to compete effectively with oxygen for reaction with the methyl radical. Based on our experience, the method should be readily applicable to most freshwater, estuarine, and coastal systems.

One major finding of this study is that SRFA exhibits a dioxygen-independent pathway of OH production that cannot be due to nitrite or nitrate photolysis or photo-Fenton chemistry. This result argues that OH is generated directly by the photolysis of CDOM (*10*, *11*) and raises the question of what this "organic" source of OH might be. Earlier work by Ronfard-Haret et al. (*25*), Brus and co-workers (*26*−*28*), and Ononye and Bolton (*29*, *30*) and more recent work by Alegria et al. (*31*) indicate that the excited triplet state of benzoquinone and certain substituted benzoquinones is capable of abstracting a hydrogen atom from water to generate OH. As quinone groups are known to exist within humic substances (*32*, *33*), excited-state hydrogen atom abstraction from water by these moieties may represent a viable explanation. Interestingly, an absorption band of benzoquinone falls in the same wavelength range in which we observe anaerobic OH generation (∼300−350 nm). Future work will be directed to testing this possible route of OH formation.

Acknowledgments

This work was supported by the Office of Naval Research (Grants N00014-95-10201 and N00014-96-10932). We thank Jordan Adelson for his assistance with atomic absorption measurements.

Literature Cited

(1) Blough, N. V. In *The Sea Surface and Global Change*; Liss, P. S., Duce, R. A., Eds.; Cambridge University Press: Cambridge, 1997; pp 383−424.
(2) Blough, N. V.; Zepp, R. G. In *Active Oxygen in Chemistry*; Foote, C. S., Valentine, J. S., Greenberg, A., Liebman, J. F., Eds.; Chapman and Hall: New York, 1995; pp 280−333.
(3) Zafiriou, O.; True, M. *Mar. Chem.* **1979**, *8*, 9−32.
(4) Zafiriou, O.; Bonneau, R. *Photochem. Photobiol.* **1987**, *45*, 723−727.
(5) Zafiriou, O.; True, M. *Mar. Chem.* **1979**, *8*, 33−42.
(6) Zepp, R.; Hoigne, J.; Bader, H. *Environ. Sci. Technol.* **1987**, *21*, 443−450.
(7) Zellner, R.; Exner, M.; Herrmann, H. *J. Atmos. Chem.* **1990**, *10*, 411−425.
(8) Faust, B. C. In *Aquatic and Surface Photochemistry*; Helz, G., Zepp, R. G., Crosby, D. G., Eds.; Lewis Publishers: Boca Raton, 1994; pp 3−38.
(9) Zepp, R. G.; Faust, B. C.; Hoigne, J. *Environ. Sci. Technol.* **1992**, *26*, 313−319.
(10) Mopper, K.; Zhou, X. *Science* **1990**, *250*, 661−664.
(11) Zhou, X.; Mopper, K. *Mar. Chem.* **1990**, *30*, 71−88.
(12) Eberhart, M.; Colina, R. *J. Org. Chem.* **1988**, *53*, 1071−1074.
(13) Kieber, D. J.; Blough, N. V. *Anal. Chem.* **1990**, *62*, 2275−2283.
(14) Blough, N. V.; Simpson, D. J. *J. Am. Chem. Soc.* **1988**, *110*, 1915−1917.
(15) Kieber, D. J.; Johnson, C. G.; Blough, N. V. *Free Radical Res. Commun.* **1992**, *16*, 35−39.
(16) Johnson, C. G.; Caron, S.; Blough, N. V. *Anal. Chem.* **1996**, *68*, 867−872.
(17) Li, B.; Gutierrez, P. L.; Blough, N. V. *Anal. Chem.* **1997**, *69*, 4295−4302.
(18) U.S. EPA. *Methods for chemical analysis of water and wastes*—*Method No. 353.2*; U.S. EPA Office of Research and Development: Washington, DC, 1979.
(19) Hatchard, C. G.; Parker, C. A. *Proc. R. Soc. London, Ser. A* **1956**, *235*, 518−536.
(20) Day, R. A.; Underwood, A. L. *Quantitative Analysis*, 3rd ed.; Prentice-Hall: New York, 1974.
(21) Kieber, D. J.; Blough, N. V. *Free Radical Res. Commun.* **1990**, *10*, 109−117.
(22) Buxton, G. V.; Greenstock, C. L. *J. Phys. Chem. Ref. Data* **1988**, *17*, 513.
(23) Neta, P. *J. Phys. Chem. Ref. Data* **1990**, *19*, 413−513.
(24) Ingold, K. U. In *L-B Numerical Data and Functional Relationships in Science and Technology, Subvol. C*; Fischer, H., Ed.; Springer-Verlag: New York, 1983; Vol. 13; pp 166−270.
(25) Ronfard-Haret, J.; Bensasson, R. *J. Chem. Soc., Faraday Trans. 1* **1980**, *76*, 2432−2436.
(26) Beck, S. M.; Brus, L. E. *J. Am. Chem. Soc.* **1982**, *104* (4), 1103−1104.
(27) Beck, S. M.; Brus, L. E. *J. Am. Chem. Soc.* **1982**, *104* (4), 4789−4792.
(28) Rossetti, R.; Brus, L. E. *J. Am. Chem. Soc.* **1986**, *108* (8), 4718−4720.
(29) Ononye, A. I.; McIntosh, A. R.; Bolton, J. R. *J. Phys. Chem.* **1986**, *90*, 6266−6270.
(30) Ononye, A. I.; Bolton, J. R. *J. Phys. Chem.* **1986**, *90*, 6270−6274.
(31) Alegria, A.; Ferrer, A.; Sepulveda, E. *Photochem. Photobiol.* **1997**, *66*, 436−442.
(32) Maximov, O. B.; Glebko, L. I. *Geoderma* **1974**, *11*, 17−28.
(33) Stevenson, F. J. *Humus Chemistry, Genesis, Composition, Reactions*; John Wiley and Sons: New York, 1982.

Received for review December 2, 1997. Revised manuscript received April 21, 1998. Accepted May 6, 1998.

ES9710417